Desalination and Water Treatment
www.deswater.com

doi: 10.1080/19443994.2013.811116

52 (2014) 6135–6144
September

Taylor & Francis
Taylor & Francis Group

Effects of electric current type and electrode configuration on the removal of Indigo Carmine from aqueous solutions by electrocoagulation in a batch reactor

Marius Sebastian Secula*, Laura Zaleschi, Corneliu Sergiu Stan, Ioan Mămăligă

Faculty of Chemical Engineering and Environmental Protection, TUIASI – Gheorghe Asachi Technical University of Iasi, Blvd. Prof. Dr. docent D. Mangeron, No. 73, 700050 Iasi, Romania
Tel. +40 232 278683; Fax: +40 232 271311; email: mariussecula@ch.tuiasi.ro

Received 15 March 2013; Accepted 24 May 2013

ABSTRACT

The aim of this study is to investigate several electrode configurations and establish the effects of alternating current (AC), alternating pulse current (APC), and direct current (DC) on an electrocoagulation (EC) process conducted in a batch reactor. Indigo Carmine (IC) was considered as pollutant model. The investigated electrode configurations consisted in aluminum/aluminum, mild steel/mild steel, and aluminum/mild steel pairs. The effects of electrode configurations and current regimes on the removal efficiency, energy consumption, electrical operating costs, and electrode dissolution rate are discussed. The most powerful electrode configuration for IC removal from aqueous solutions by EC consisted in an anode of mild steel and a cathode of aluminum. EC operated in AC mode resulted in low efficiencies in any electrode configuration of those considered. Contrariwise, APC provided higher performance to the EC process in comparison with DC. Also, it led to higher dissolution rates in case of aluminum electrodes and to a more stable removal of dye when mild steel anode was employed. Energy-Dispersive X-Ray spectroscopy, Fourier transform infrared (FTIR), and scanning electron microscopy (SEM) analytical methods were used to characterize the sludge separated by sedimentation and flotation in case of EC in APC mode using Al–Fe configuration. Thus, it was shown that IC dye was adsorbed on aluminum and iron hydroxides.

Keywords: Alternating pulse current; Dissolution rate; Electrical operating costs; Electrocoagulation; Indigo Carmine

---

1. Introduction

Electrocoagulation (EC) is known as a fast, reproducible, eco-friendly and cheap method for wastewater treatment [1,2]. However, it has never been accepted as a mainstream method [3,4] though EC technique provides low costs for wastewater treatment without any need for additional chemicals [5–10].

The disadvantages of EC are claimed to consist mainly in high-energy consumption [2,11,12], the formation of an impermeable layer on the cathode surface resulting in an important loss of efficiency

---

*Corresponding author.

[3,9] and high conductivity is required for wastewater treatment [13]. Nevertheless, operated under optimal current densities, EC might be much cheaper than most of advanced wastewater treatment methods. The hindrance due to the formation of impermeable layer on the cathode might be solved by using alternating pulse current (APC) [3,12,14]. Also, dyeing effluents contain high chloride content, and thus, there is no need to be added externally [15,16].

EC is a complex process characterized by a multitude of mechanisms that operate synergistically in order to remove pollutants from water [9,17]. EC mechanisms may involve oxidation, reduction, decomposition, deposition, coagulation, absorption, adsorption, precipitation, and flotation [8]. Although the mechanisms involved in EC process are yet not fully understood [18], according to the current theory of EC, a coagulant is generated in situ by electrolytic oxidation of a soluble electrode, and ions are formed by water electrolysis at the cathode [5,10,19]. Creating a favorable chemical/physical environment for the destabilization of a large range of pollutants, the most widely used electrode materials in EC process are aluminum (Al) and iron (Fe) [8,10,20–23].

In case of aluminum electrodes, Al^{3+} is produced, which generates further $Al(OH)^{2+}$, $Al(OH)_2^+$, gelatinous $Al(OH)_3$ that is finally polymerized to $Al_n(OH)_{3n}$ [24]. Anodic dissolution of iron leads to the formation of $FeOH^{2+}$, $Fe(OH)_2$, $Fe(OH)_2^+$, $Fe(OH)_3$, $Fe(OH)_4^-$, and FeO(OH) [19]. Then, charged particles present in wastewater are transformed into amorphous precipitates, absorbed on the flocs of metallic hydroxides or complexed (where the pollutant acts as a ligand and is chemically bind by hydrous iron) and removed by sedimentation and/or flotation [4,24,25].

Based on the consumptions of electrical energy and electrode material, electrical operational costs of EC represent an important factor for judging the feasibility of the process. However, only a few works approached the economic aspects [26] of EC technique. Excepting the works of Keshmirizadeh et al. [24] and Eyvaz et al. [27], according to our knowledge, no other studies concerning operating costs of EC in APC mode have been reported so far.

In a previous study, Secula et al. [28] reported an experimental study of IC removal from aqueous solutions by EC under direct current (DC) regime. IC was considered as dye model due to it is a highly water-soluble acid dye [29] used in the textile industry for the dyeing of polyamide and protein fibers [28,30].

Our prior work was focused especially on the influence of several operating parameters such as current density, initial pH, initial dye concentration, electrolysis time, electrolyte support concentration on the decolorization process.

The main goal of this work consists in the investigation of the effect of several electrode configurations and current regimes on the removal of an anionic dye from aqueous solutions by EC in a batch reactor in relation to removal efficiency, energy, and material consumption and electrical operating costs.

2. Experimental

2.1. Materials

Indigo Carmine (IC) (known also as Acid Blue 74 or Food Blue 1 or FD & C Blue 2 (CASRN 860-22-0)) is a dark blue, water-soluble powder. The molecular formula of the dye is $C_{16}H_8O_8N_2S_2Na_2$ and its molecular weight is $466.36\,g\,mol^{-1}$. Full description of the molecular structure of IC has been presented in [31].

Solutions of IC of 1 L volume were prepared fresh before each experimental run by dissolving precisely weighted amounts of dye (purchased from Sigma Aldrich) in ultrapurified water (18.2 MΩ cm at 25°C, Barnstead Easypure II Thermo Scientific water purifying system).

To adjust the solution conductivity, $1.5\,g\,L^{-1}$ NaCl (A.R. Lach-Ner, Neratovice, Czech Republic) was dissolved into dye synthetic solutions [28].

2.2. Electrocoagulation experiments

Fig. 1 shows a picture of the experimental set-up used in this study.

A 1-L glass vessel was used as EC cell. This is provided with electrode fixing channels on two opposing lateral walls. The anode and cathode were positioned vertically and fixed between the channels of EC cell at a distance of 3 mm one from another. Sheet electrodes of aluminum and mild steel of similar surface areas were employed in order to investigate several electrode configurations. The effective electrode area was $183\,cm^2$. When the EC reactor was operated in DC or alternating current (AC) (50 Hz) mode, the electrodes were connected directly to a digital DC/AC power supply. In case of APC mode, the polarity changer was employed in the electrical circuit. A DRA1 k AC/DC power supply (AC mode: 0–10 A, 0–150 V; 1–550 Hz; DC mode: 0–4.5 A, 0–150 V) Matsusada Precision Inc, Japan was used. The electrodes were polished with emery paper of various grades, washed with dilute H_2SO_4 and then with distilled water before each run. After drying, electrodes were weighed before and after EC by means of an Acculab

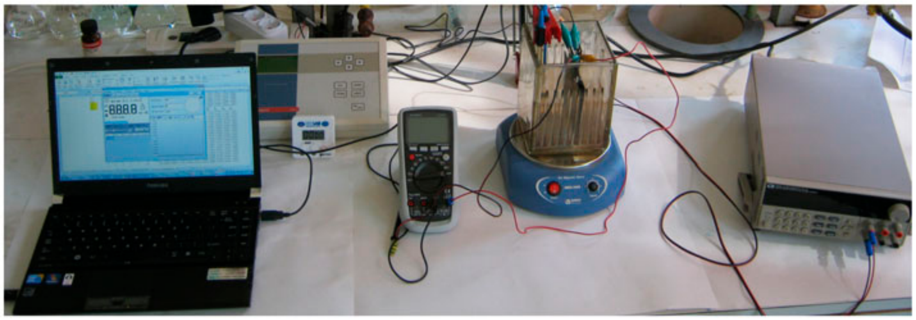

Fig. 1. Experimental set-up of EC operated in DC regime.

ATL-224-I analytical digital balance (accuracy 0.1 mg). All the runs were performed at room temperature of 25 ± 0.5˚C.

The experiments were carried out in a batch mode. In each run, 1,000 cm^3 IC model wastewater solution was placed into the EC cell, and a gentle agitation was ensured along the run to get a homogenous suspension by means of a BOECO MMS 3000 magnetic stirrer. The current density was set to a desired value, and then coagulation was started.

For each decolorization analysis, less than 5 cm^3 of sample was taken, let to settle for 1 h and centrifuged at 4000 RPM by means of a BOECO S8 EBA20 centrifuge, and then analyzed. For all the experiments, a maximum volume of 60 cm^3 was taken for the assessment of the treatment progress.

A VC530 Voltcraft data logging multimeter connected to a PC was used to measure (one reading per second) the cell voltage as presented in Fig. 5(b). The solution pH and conductivity were measured by means of a C863 Consort multiparameter analyzer that was also connected to a PC.

The color removal efficiency (RE, %) was calculated from:

$$\mathrm{RE} = \frac{C_0 - C}{C_0} \times 100 \tag{1}$$

where C_0 is the concentration of dye before EC ($\mathrm{mg\,L^{-1}}$), and C is the concentration of dye after t minutes of EC ($\mathrm{mg\,L^{-1}}$).

The runs were carried out in three replications used to compute the mean value and the standard deviation parameters. The low values determined for standard deviation suggest a high reproducibility of the results.

2.3. Determination of electrical operating costs

The energy consumption related to the amount of removed dye, named herein further as unit energy demand (UED) [32], was determined. Since the experiments were carried out under galvanostatic mode, i.e. the current intensity was kept constant, and cell voltage varied during EC, the following relationship was used (2):

$$\mathrm{UED} = I \times \int_0^t U \times \mathrm{d}t \Big/ \left(1,000 \times V \times C_0 \times \frac{\mathrm{RE}_t}{100}\right) \tag{2}$$

where UED is the unit energy demand, ($\mathrm{kWh\,kg^{-1}}$); U – cell voltage, (V), I – current intensity, (A), t – time, (h), C_0 – initial concentration of dye, ($\mathrm{kg\,m^{-3}}$), V – volume of treated solution, ($\mathrm{m^{-3}}$), RE_t – removal efficiency at time t (%).

The electrical operational costs of EC process can be calculated by taking into account the amount of energy consumption and consumed materials (Eq. (3)) [21]:

$$EOC = EEC + MC = UED \times EEP + AMC \tag{3}$$

where EOC is the electrical operating cost, (\$ $\mathrm{kg^{-1}}$ of dye removed); EEC – electrical energy consumption, (\$ $\mathrm{kg^{-1}}$ of dye); EEP – electrical energy price, (\$ $\mathrm{kWh^{-1}}$); AMC – anode material consumption, (\$ $\mathrm{kg^{-1}}$).

The cost of the consumed electrode material can be estimated based on Faraday's law by means of Eq. (4) [25]:

$$AMC = \frac{I \times t \times A}{n \times F} \times \frac{AMP}{V \times C_0 \times \frac{\mathrm{RE}_t}{100}} \tag{4}$$

where AMC is the cost of anode material consumed during EC, (\$ $\mathrm{kg^{-1}}$ of dye removed); I – current intensity, (A); t – time, (s); n – number of electrons involved in oxidation/reduction reaction; F – Faraday's constant, ($\mathrm{C\,mol^{-1}}$); A – atomic mass of electrode material, ($\mathrm{g\,mol^{-1}}$); V – volume of treated solution, ($\mathrm{m^{-3}}$); C_0 – initial concentration of dye, ($\mathrm{kg\,m^{-3}}$), AMP – anode material price, (\$ $\mathrm{g^{-1}}$).

The electrode material cost was computed based on the amount dissolved during EC, which was determined by weighing the electrodes before and after EC.

In order to determine these operational costs, economic data were gathered from the EU market in 2013. Thus, the electrical energy price for industrial use was averaged to 0.1 (\$ kW h^{-1}), while mild steel and aluminum sheets were estimated at 1 and 2 (\$ kg^{-1}), respectively.

2.4. Analytical methods

The concentration of IC was determined at $\lambda = 612$ nm using a Thermo Scientific Helios Epsilon UV/VIS spectrophotometer.

SEM and Energy-Dispersive X-Ray spectroscopy (EDX) analysis of the resulted sludge by flotation and sedimentation was performed with a FEI Quanta 200 SEM provided also with an Apollo X-SDD detector. FTIR spectra of the resulted sludge by flotation and sedimentation were recorded in the range 400–4,000 cm^{-1} using a FTIR DIGILAB-FTS 2000 Spectrometer provided with an ATR (ZnSe) device, according to KBr pellet method.

3. Results and discussion

3.1. Effect of electric current type

3.1.1. Alternating current vs. direct current

Fig. 2 shows the evolutions of removal efficiency during EC in DC and AC regimes, respectively, for pairs of aluminum electrodes and iron-based electrodes. In this series of experimental runs, the effects of DC and AC (50 Hz) regimes on the EC of IC aqueous solutions were investigated at a constant current density of 27.28 A m^{-2}.

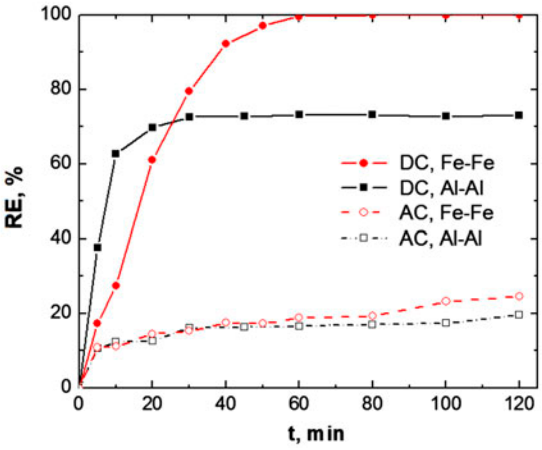

Fig. 2. Evolution of IC removal efficiency by EC in DC and AC mode in two electrode configuration, Al–Al and Fe–Fe ($C_i = 50$ mg L^{-1}; $j = 27.28$ A m^{-2}; pH$_i$ = 5.5).

In both cases, the decolorization obtained by EC in AC (50 Hz) mode is much weaker than that achieved by EC operated in classical DC mode. Although at the beginning of the EC process, aluminum electrochemical dosing in DC mode results in a faster decolorization, RE reaches a plateau at 76% after 30 min of electrolysis. Though iron-based EC in DC mode is slower in comparison with aluminum electrode configuration, an almost complete removal of IC is achieved after 60 min.

EC operated in AC mode is known to delay the normal mechanisms of electrode corrosion that are experienced in DC regime [13]. In our study, this is supported by the relatively low amount of electrode material dissolved. Thus, in case of Al–Al electrode configuration, the dissolution rate of aluminum was approximately 16% that of the theoretical dissolution rate calculated according to Farraday's law. This is in good agreement with the results reported by Sabeva and Dobrewsky [33] according to which, the dissolution rate of aluminum at current densities lower than 100 A m^{-2} is about 15% of the theoretical dissolution rate and increases to less than 70% at current density values of about 1,000 A m^{-2}.

3.1.2. Alternating rectangular pulse current vs. direct current

Fig. 3 presents the evolutions of removal efficiency and UED during iron-based EC operated in DC mode and APC mode at different periods (60, 300, 540 Hz^{-1}).

In terms of RE, EC operated in APC mode is relatively close to EC operated in DC mode. As can be noticed, RE is slightly improved at the highest period of APC considered, while at low periods, the removal of dye is slower. In terms of UED, the energy consumption is significantly diminished with the increase in APC period. Taking into account very low values of current density, when electrophoretic transport is relatively slow, we consider that it is possible that EC in APC mode is slightly more favorable at high periods due to the charged particles have enough time to reach at the coagulant formed near the electrode. The favorable influence on the UED is given by the significant decrease in voltage during operation in APC mode especially at high values of APC period, which leads to lower energy consumption.

3.2. Effect of electrode configuration

In order to pinpoint this effect, it was considered that a high value of current density will amplify the differences that were supposed to occur. Therefore, the runs were carried out at a current density of 109.14 A m^{-2}. According to the previous study of Secula et al. [28], an acid initial pH of IC aqueous solution favors the decolorization process. For this series of runs, before EC, the pH of dye solutions was adjusted to a value of 3.

EC tests were carried out on aqueous solutions containing 1,000 mg L^{-1} of IC. Fe–Fe, Al–Al, and Al–Fe configurations were investigated under DC and APC (300 Hz^{-1}) mode. Fig. 4 shows the evolutions of RE for the considered electrode configurations and current regimes under the experimental conditions specified in figure caption.

The use of Al–Al electrode configuration in EC of IC aqueous solutions under either DC or APC mode resulted in a relatively poor separation of dye. Thus, EC operated in DC mode leads to a RE of 59.65% after 2 h (Fig. 4(a)), while in case of EC in APC (300 Hz^{-1}) mode, a RE of 57.67% was achieved after 90 min of electrolysis (Fig. 4(b)). The reason why the EC in Al–Fe (Al - anode; Fe - cathode) configuration in DC mode is even less effective than Al–Al configuration lies in the lower amount of Al^{3+} ion dissolved. Since there is no cathode dissolution in Al–Fe configuration, the total dissolution rate of coagulant is approximately 29% lower. The values of dissolution rate of the investigated electrode configurations are presented in Table 1.

EC using Fe–Fe configuration, in DC and APC mode, produces maximum RE values of 80.01 and 84.34%, respectively, after 45 min. After 2 h of EC operated in DC mode, RE decreases to 62.52 % after 45 min (Fig. 4(a)). This was not observed in case of APC mode when is reached a plateau in RE at about

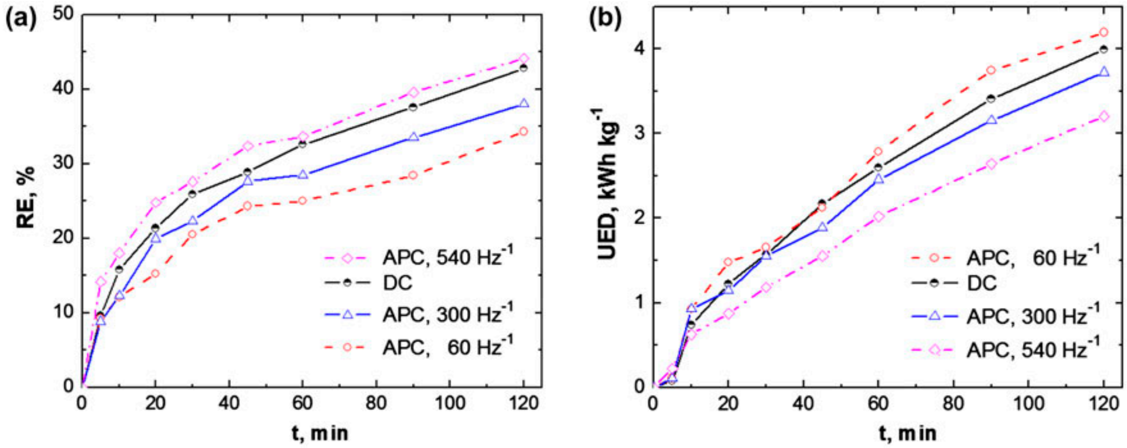

Fig. 3. Evolution of RE (a) and UED (b) at EC in DC and APC mode at different periods, Fe–Fe electrode configuration ($C_i = 50$ mg L^{-1}, $j = 2.73$ A m^{-2}, pH$_i$ = 5.5).

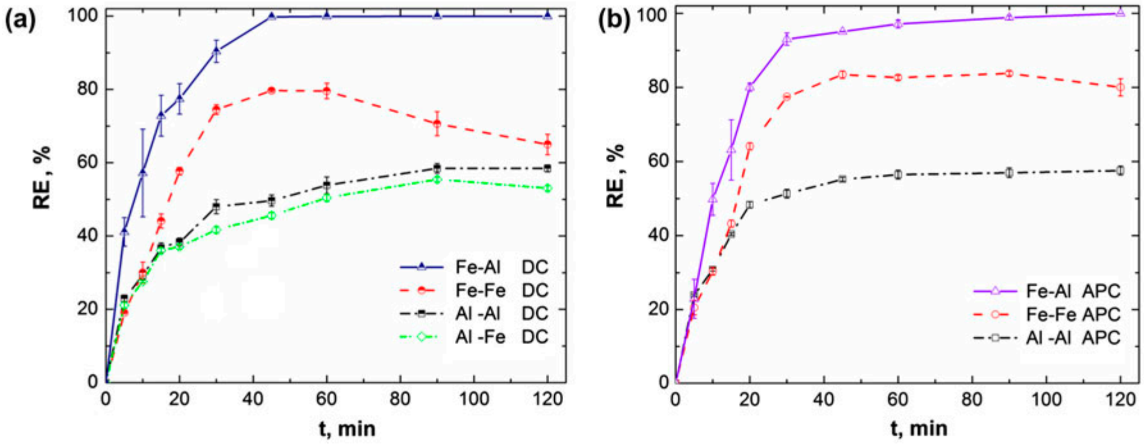

Fig. 4. Evolution of RE at EC in (a) DC and (b) APC mode, respectively, using different electrode configurations ($C_i = 1{,}000$ mg L^{-1}, $j = 109.14$ A m^{-2}, pH$_i$ = 3).

84% (Fig. 4(b)). When DC is applied, anionic IC molecules are attracted by the cathode, which is covered during electrolysis and thus the mechanism of coagulation becomes affected. In addition, molecules of dye begin to dissolve into the aqueous solution after 45 min. As the flocs formed with iron hydroxides are relatively stable, and due to the diminution in RE is limited, it is supposed that the molecules of dye covering the cathode surface are those which are dissolved.

Remarkable results were achieved in case of Fe–Al configuration. For instance, in DC mode (Fig. 4(a)), EC presents twofold values of RE after 5 and 10 min of electrolysis, and RE reaches 99.85% at 45 min. In APC mode (Fig. 4(b)), a RE value of 93.04% is obtained after only 30 min and then the decolorization rate decreases sharply, the complete removal of dye, i.e. 99.96%, being achieved after 2 h of electrolysis.

Recently, Keshmirizadeh et al. [24] reported the removal of Cr(VI) from aqueous solutions by EC in APC mode using Al–Fe configuration. They claimed that the main effects of applying APC compared with DC consisted in an improved turbidity and water recovery (92% in APC vs. 50% in DC mode). However, in the investigations presented in this study, the percent of water recovery by sedimentation exceeded 85%, while the filtration of effluents ensured water recoveries of about 95% for both types of current.

Fig. 5(a) shows the evolution of energy consumptions for the considered electrode configurations.

Having in view the low interelectrode distance employed in the investigations reported in this work, it was observed that for EC using Fe–Al configuration in DC, at high values of current density, it is formed a high resistive spongious layer between the electrodes (insert digital image in Fig. 5(a)) which leads to a sharp increase in energy consumption. In Fig. 5(b), it can be seen how after 30 min of electrolysis, the resistive layer begins to form between the electrodes (Fe - anode; Al - cathode) thus resulting in a sharp increase in the voltage of current applied. This phenomenon can be avoided by applying APC which allows a "self-cleaning" of electrodes. Due to the change of electrode polarity, the direction of electrophoretic transport of charged particles is also changed. Thus, the sludge accumulating in the interelectrode region is removed and the overconsumption of electrical energy is avoided.

The use of Fe–Fe configuration during EC resulted in the lowest energy consumption independently on the current type applied, while Al–Al configuration provided relatively high-energy consumption especially under DC regime.

Taking into account that the costs related to electrode material and electrical energy vary from one geographical area to another and are related to the evolution of prices in the markets, beside energy consumption and UED, we present also the values of dissolution rate (standing at the basis of EOC determination) for each considered electrode configuration (Table 1).

In case of iron-based material, the values of dissolution rate are significantly higher in comparison with those obtained in case of aluminum electrodes. This is due to there are three electrons involved in the electrochemical dissolution of Al electrode, and only two electrons in case of Fe. Compared with DC mode, Al–Al electrode configuration provides significantly higher amounts of Al^{3+} ions when EC is operated in APC mode. Not surprisingly, the electrode configuration of Al–Fe in APC mode results in a total dissolution rate significantly lower than in DC mode. This is

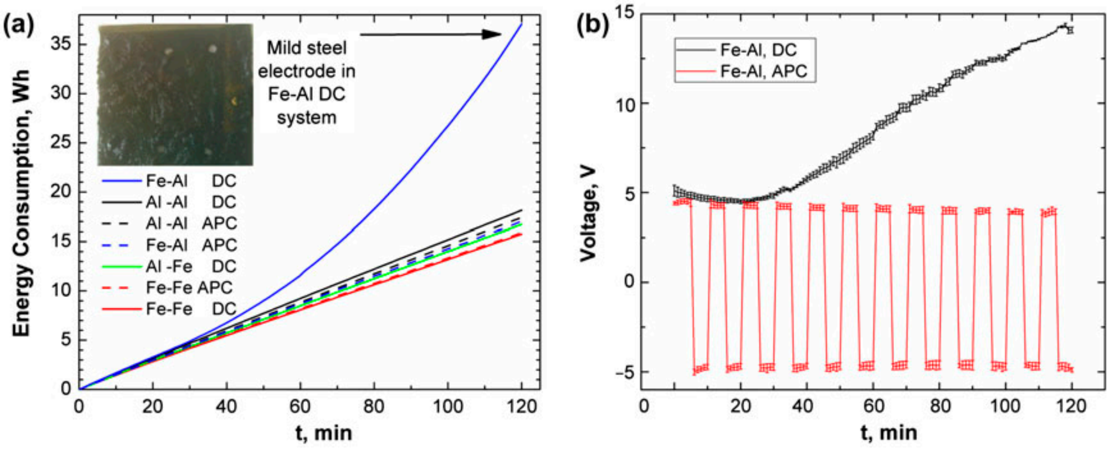

Fig. 5. Evolution of energy consumption using different electrode configurations (a); and voltage evolution for Fe–Al Fe - anode; Al - cathode) configuration in DC mode (b).

Table 1
Dissolution rate values of the considered electrode configurations ($C_i = 1{,}000\,\text{mg}\,\text{L}^{-1}$, $j = 109.14\,\text{A}\,\text{m}^{-2}$, $\text{pH}_i = 3$).

Electrode configuration	Current type	Anode*		Cathode*	
		Material	Dissolution rate $\times 10^2$ $\text{g}\,\text{s}^{-1}\,\text{m}^{-2}$	Material	Dissolution rate $\times 10^2$ $\text{g}\,\text{s}^{-1}\,\text{m}^{-2}$
Al–Al	DC	Al	1.2208 ± 0.0062	Al	0.4752 ± 0.0314
Al–Al	APC	Al	1.2710 ± 0.0239	Al	1.2825 ± 0.0265
Fe–Fe	DC	Fe	3.2257 ± 0.0017	Fe	0
Fe–Fe	APC	Fe	1.5762 ± 0.0032	Fe	1.5747 ± 0.0021
Al–Fe	DC	Al	1.2204 ± 0.0045	Fe	0
Al–Fe	APC	Al	1.2681 ± 0.0850	Fe	1.5028 ± 0.0178
Fe–Al	DC	Fe	3.1242 ± 0.0730	Al	0.7206 ± 0.0685

*In case of APC regime, electrode role at the beginning of EC.

explained on one hand by the cathodic dissolution of Al and on the other hand Fe in APC mode is generated only for only a half of the electrolysis time.

Fig. 6 shows a comparative diagram where four different indicators of EC are emphasized as a function of electrode configuration operated in DC and APC modes, respectively.

The configuration based only on aluminum as anode results in relatively poor RE and high UED and EOC values. On the contrary, iron-pairs configurations give relatively good RE values and lower UED and EOC values. The best performance for IC separation was achieved using Fe–Al in DC mode and Al–Fe in APC mode. As already mentioned above, due to the very high-energy consumption and fouling, Fe–Al in DC mode is not a feasible solution. On the contrary, EC using Al–Fe operated in APC mode provides both very good RE and low UED.

UED increases during EC mainly due to the increment in energy consumption, but also due to the diminution of dye concentration. As Al–Al configurations provided among the weakest RE and the highest energy consumption, the values of UED underline the relatively low feasibility of this configuration. However, in the first 60 min of EC, aluminum-based configuration employed in APC mode provided a rather lower UED values in comparison with those obtained in DC mode, which means that a lower amount of energy is required to remove a certain amount of dye. Al–Fe (Al - anode; Fe - cathode) configuration operated in DC mode presented the most unfavorable (highest) UED values.

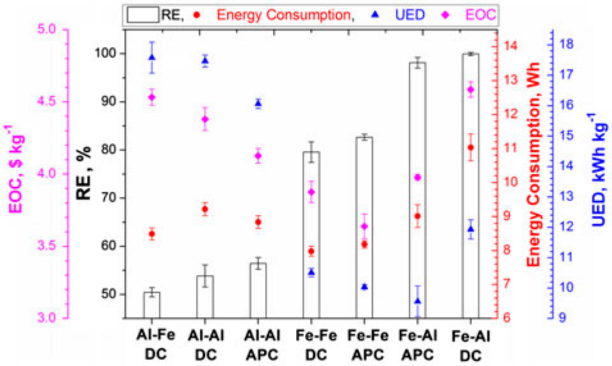

Fig. 6. Effect of electrode configurations on EC of IC aqueous solution in DC and APC mode respectively ($C_i = 1{,}000\,\text{mg}\,\text{L}^{-1}$, $j = 109.14\,\text{A}\,\text{m}^{-2}$, $\text{pH}_i = 3$, $t = 60\,\text{min}$).

On the contrary, having relatively good RE values and low-energy consumption, Fe–Fe configurations ensured also low values of UED. The use of APC mode resulted in even lower UED values.

EC using Fe–Al (Fe-anode; Al-cathode) configuration in DC mode provided the fastest removal of dye. Nevertheless, in terms of UED, DC regime proves to be more energy consuming than APC regime.

In terms of EOC, one of the cheapest electrode configurations in relation to the amount of dye removed is represented by Fe–Fe, though, Fe–Al in DC mode resulted to be the cheapest configuration by far, this is not quite a feasible one due to the fouling of the electrodes.

Taking into account the promising results obtained with Al–Fe configuration operated in APC mode in order to remove IC from aqueous solutions, the optimization of this EC process in terms of RE, UED, and EOC is considered for a future work.

3.3. FTIR, EDX, and SEM studies of the sludge formed in Al–Fe configuration in APC mode

The sludge separated by flotation and sedimentation was characterized by SEM technique as shown in Fig. 7.

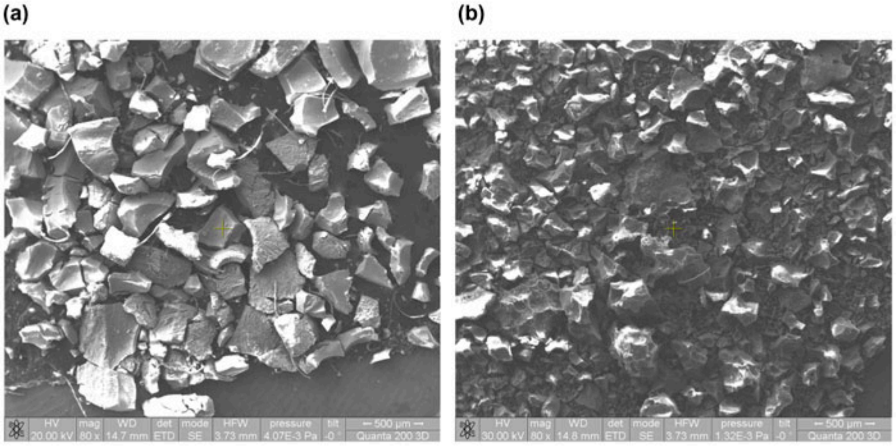

Fig. 7. SEM images of (a) sedimentation and (b) flotation sludge.

Table 2
Elemental compositions of (a) sedimentation and (b) flotation sludge

Element	Weight percent							
	C	N	O	Na	Al	S	Cl	Fe
Sedimentation sludge	10.16	9.28	39.03	0.21	14.3	0.26	1.7	25.06
Flotation sludge	12.77	11.34	43.59	0.38	15.62	1.8	0.86	13.63

As expected, the sludge particles separated by flotation at the surface of the effluent are significantly smaller than those deposited at the bottom of the EC cell.

Energy-dispersive analysis of X-rays was used to analyze the elemental constituents of IC-adsorbed aluminum and iron hydroxides separated by sedimentation and flotation.

Table 2 presents the elemental composition of the sludge separated by flotation at the surface, and by sedimentation.

The elements specific to IC, such as C, N, Na, and S are found in higher percentages in the flotation sludge pinpointing that this was the main separation process under the considered experimental conditions. Also, it can be observed that Fe can be found in a significantly higher percentage in the sedimentation sludge. According to the observations during EC process conducted at a current density of 109.14 A m^{-2}, most of the IC dye was separated by flotation.

Fig. 8 presents the FT-IR spectrum of the sludge separated by sedimentation or flotation.

The sharpest and strongest peaks at 3460.29 and 2360.86 cm^{-1} are due to the O–H stretching and vibration, bonding O–H stretching in the hydroxides structures, respectively. The peak at 1637.56 cm^{-1} is assigned to the bending vibration of H–O–H. The peaks in the range 1,030–1,000 cm^{-1} are assigned to M-O-H bending. Considering that most of the dye was separated by flotation during EC process, the peak at 1105.21 cm^{-1} in case of the flotation sludge spectrum is related to the S=O bonds characteristic to IC (Fig. 8, line (b)).

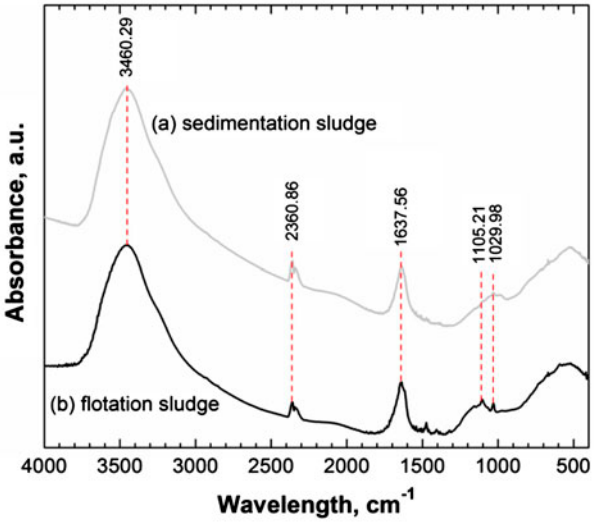

Fig. 8. FTIR spectra of (a) sedimentation and (b) flotation sludge.

4. Conclusion

The purpose of the present work was to provide more insights into the effects of AC and alternating rectangular pulse current on the dissolution rate of electrode material, removal efficiency, energy consumption, and electrical operating costs.

Thus, there have been established the effects of several electrode configurations and applied current type on the removal of IC from aqueous solutions by EC in a batch reactor.

It was found that applying AC (50 Hz) results in relatively poor removal efficiencies compared with DC. However, APC mode leads to higher dissolution rate values in case of aluminum pair electrode configuration, more stable removal of dye in case of iron-based electrode configurations, and a complete decolorization with the lowest UED when aluminum/iron configuration was employed.

Among the pairs of aluminum or mild steel plan electrodes and coupling of both electrode materials, the best performance was achieved with Fe–Al electrode configuration. Although in case of the latter electrode configuration, the DC mode provided the fastest removal of dye mainly due to the high amount of metal ions dissolved, APC proved to be an important solution in order to make the EC process using this configuration a feasible one.

Also, it was shown that periods higher of 5 min of APC applied to EC using Fe–Fe electrode configuration leads to higher removal efficiencies. Moreover, UED values decreases with increasing the period of APC.

Based on FTIR and EDX analytical methods, it was shown that in case of Fe–Al electrode configuration in APC mode IC was adsorbed on aluminum and iron hydroxides.

Acknowledgment

This study was supported by CNCSIS-UEFISCSU, project number PN II-RU No. 52/2010, COD 44.

References

[1] I. Ali, T.A. Khan, M. Asim, Removal of arsenate from groundwater by electrocoagulation method, Environ. Sci. Pollut. Res. 19 (2012) 1668–1676.

[2] A. Kumar, P. Choudhary, P. Verma, A comparative study on the treatment methods of textile dye effluents, J. Chem. Pharm. Res. 4 (2012) 763–771.

[3] P.K. Holt, G.W. Barton, C.A. Mitchell, The future for electrocoagulation as a localised water treatment technology, Chemosphere 59 (2005) 355–367.

[4] R. Katal, H. Pahlavanzadeh, Influence of different combinations of aluminum and iron electrode on electrocoagulation efficiency: Application to the treatment of paper mill wastewater, Desalination 265 (2011) 199–205.

[5] N. Balasubramanian, T. Kojima, C.A. Bashac, C. Srinivasakannan, Removal of arsenic from aqueous solution using electrocoagulation, J. Hazard. Mater. 167 (2009) 966–969.

[6] D. Belhout, D. Ghernaout, S. Djezzar-Douakh, A. Kellil, Electrocoagulation of a raw water of Ghrib Dam (Algeria) in batch using aluminium and iron electrodes, Desalin. Water Treat. 16 (2010) 1–9.

[7] S. Aoudj, A. Khelifa, N. Drouice, M. Heciniab, HF wastewater remediation by electrocoagulation process, Desalin. Water Treat. 51 (2013) 1596–1602.

[8] J.R. Parga, M. Rodriguez, V. Vazquez, J.L. Valenzuela, H. Moreno, Recovery of silver and gold from cyanide solution by magnetic species formed in the electrocoagulation process, Miner. Process. Extract. Metall. Rev. 33 (2012) 363–373.

[9] S. Vasudevan, J. Lakshmi, G. Sozhan, Studies on the removal of arsenate from water through electrocoagulation using direct and alternating current, Desalin. Water Treat. 48 (2012) 163–173.

[10] M.C. Wei, K.S. Wang, C.L. Huang, C.W. Chiang, T.J. Chang, S.S. Lee, S.H. Chang, Improvement of textile dye removal by electrocoagulation with low-cost steel wool cathode reactor, Chem. Eng. J. 192 (2012) 37–44.

[11] Y. Avsar, U. Kurt, T. Gonullu, Comparison of classical chemical and electrochemical processes for treating rose processing wastewater, J. Hazard. Mater. 148 (2007) 340–345.

[12] D.L. Cocke, M.Y.A. Mollah, P. Morkovsky, J.A. Gomes, M. Kesmez, J.R. Parga, Fundamentals, present and future perspectives of electrocoagulation, J. Hazard. Mater. 114 (2004) 199–210.

[13] M.Y.A. Mollah, R. Schennach, J.R. Parga, D.L. Cocke, Electrocoagulation (EC) – science and applications, J. Hazard. Mater. 84 (2001) 29–41.

[14] H. Ayedi, G. Mouedhen, M. Feki, M. Petris, Behavior of aluminium electrodes in electrocoagulation process, J. Hazard. Mater. 150 (2008) 124–135.

[15] T. Ölmez, I. Kabdasli, O. Tünay, The effect of textile industry dyebath additive EDTMPA on color removal characteristics by ozone oxidation, Water Sci. Technol. 55 (2007) 145–153.

[16] P.V. Nidheesh, R. Gandhimathi, S.T. Ramesh, Degradation of dyes from aqueous solution by Fenton processes, Environ. Sci. Pollut. Res. 20 (2013) 2099–2132.

[17] I. Kabdasli, B. Vardar, I. Arslan-Alaton, O. Tünay, Effect of dye auxiliaries on color and COD removal from simulated reactive dyebath effluent by electrocoagulation, Chem. Eng. J. 148 (2009) 89–96.

[18] C. Noubactep, A. Schöner, Metallic iron for environmental remediation: Learning from electrocoagulation, J. Hazard. Mater. 175 (2010) 1075–1080.

[19] G. Mouedhen, M. Feki, M. De Petris-Wery, H.F. Ayedi, Electrochemical removal of Cr(VI) from aqueous media using iron and aluminum as electrode materials: Towards a better understanding of the involved phenomena, J. Hazard. Mater. 168 (2009) 983–991.

[20] A. Akyol, Treatment of paint manufacturing wastewater by electrocoagulation, Desalination 285 (2012) 91–99.

[21] M.Y.A. Mollah, P. Morkovsky, J.A.G. Gomes, M. Kesmez, J. Pargad, D.L. Cocke, Fundamentals, present and future perspectives of electrocoagulation, J. Hazard. Mater. 114 (2004) 199–210.

[22] D. Reddithota, A. Yerramilli, Electrocoagulation: A cleaner method for treatment of Cr(VI) from electroplating industrial effluents, Ind. J. Chem. Technol. 14 (2007) 240–245.

[23] İ.A. Şengil, A. Özdemir, Simultaneous decolorization of binary mixture of blue disperse and yellow basic dyes by electrocoagulation, Desalin. Water Treat. 46 (2012) 215–226.

[24] E. Keshmirizadeh, S. Yousefi, M.K. Rofouei, An investigation on the new operational parameter effective in Cr(VI) removal efficiency: A study on electrocoagulation by alternating pulse current, J. Hazard. Mater. 190 (2011) 119–124.

[25] F.R. Espinoza-Quinones, M.M.T. Fornari, A.N. Módenes, S.M. Palácio, F.G. da Silva Jr, N.A.D. Szymanski, N. Kroumov, D. E.G. Trigueros, Pollutant removal from tannery effluent by electrocoagulation, Chem. Eng. J. 151 (2009) 59–65.

[26] M. Bayramoglu, M. Kobya, O.T. Can, M. Sozbir, Operating cost analysis of electrocoagulation of textile dye wastewater, Sep. Purif. Technol. 37 (2004) 117–125.

[27] M. Eyvaz, M. Kirlaroglu, T.S. Aktas, E. Yuksel, The effects of alternating current electrocoagulation on dye removal from aqueous solutions, Chem. Eng. J. 153 (2009) 16–22.

[28] M.S. Secula, I. Cretescu, S. Petrescu, An experimental study of indigo carmine removal from aqueous solution by electrocoagulation, Desalination 277 (2011) 227–235.

[29] B. Adinew, Textile effluent treatment and decolorization techniques – a review, Chem.: Bulgarian J. Sci. Edu. 21 (2012) 434–456.

[30] G. Fischer-Colbrie, J. Maier, K.H. Robra, G.M. Guebitz, in: E. Lichtfouse, J. Schwarzbauer, D. Robert (Eds.), Environmental Chemistry: Green Chemistry and Pollutants in Ecosystems, Springer-Verlag, Berlin Heidelberg, Germany, 2005, p. 289.

[31] M.S. Secula, B. Cagnon, T. Ferreira de Oliveira, O. Chedeville, H. Fauduet, Removal of acid dye from aqueous solutions by electrocoagulation/GAC adsorption coupling: Kinetics and electrical operating costs, J. Taiwan Inst. Chem. Eng. 43 (2012) 767–775.

[32] M.S. Secula, I. Cretescu, S. Petrescu, Electrocoagulation treatment of sulfide wastewater in a batch reactor: Effect of electrode material on electrical operating costs, Environ. Eng. Manage. J. 11 (2012) 1485–1491.

[33] E. Sabeva, I. Dobrewsky, The effect of the type of electric current on the cathodic corrosion of aluminium, J. Appl. Electrochem. 20 (1990) 986–988.